THE CHALK RIVER ELECTRON TEST ACCELERATOR

by
J.S. Fraser, S.H. Kidner, J. McKeown and G.E. McMichael

Chalk River Nuclear Laboratories
Chalk River, Ontario, Canada

Introduction

A 1 GeV proton linear accelerator operated at 100% duty factor and high beam loading is a possible accelerator for electronuclear production of fissile materials (1). Conceptually, such a machine would be similar to the ING reference design (2) but with higher beam loading. Experiments on the low energy section of such a linac are described in another paper at this conference (3). The high energy section could be a side-coupled cavity structure patterned on the LAMPF design. A test accelerator is being constructed for use with electrons (β=1) to model the behaviour of intermediate energy protons (β=0.2 to 0.8). This accelerator will provide a facility for exploring such questions as (a) the transverse beam instability at high currents, (b) tank frequency control with high beam loading and high power dissipation and (c) the functioning of fast shutdown systems. Potential applications of this Electron Test Accelerator (ETA) are foreseen in large volume radiation processing.

The accelerator comprises a gun, a buncher, a graded-β pre-accelerator and a main accelerator section with β=1. The accelerator sections operate at 805 MHz, each driven by a 100 kW klystron. The output beam is bent through 90° into a high power beam dump. An isometric view of the complete installation is shown in Fig. 1. At the time of writing, the injector and pre-accelerator sections are complete and have been operated. The tuning of the second accelerator section is complete and vacuum fittings are being made. The high power beam dump is complete and has been installed.

The design objective of the first phase of the experiment is to accelerate a beam of 15 mA to 4 MeV. The available components are capable of operation at 50 mA of beam with an average energy of 2.8 MeV. The design objective of several hundred mA at 4 MeV would require a larger rf power source possibly operated in a long-pulse mode. Although in principle ETA does not differ from medium energy research accelerators, specific problems arise because of this high average current and power. The transport sensing system must be able to respond quickly to any beam disturbance and the control systems must be designed to respond with corrective action or effect shutdown in microseconds.

Major Components

Gun

The electron source is a three-element gun capable of delivering a beam of up to 200 mA at 100 keV. The intermediate electrode is normally operated at a potential appropriate to Pierce-gun design but its function is to provide a fast control facility for the stabilization of accelerator beam current. The beam diameter from the gun anode has been measured up to 60 mA and found to be less than 1.5 mm 54 cm downstream. Above 60 mA, the beam scanner used was incapable of absorbing the beam power without damange.

Rf System

The klystrons in use are a VA-853 modified to operate at fixed frequency with 53% efficiency and a VA-3076 developmental 65% efficiency tube. A fast protect system either removes the drive power or crowbars the HT in a few microseconds. A more detailed discussion of the rf system is given in ref. (4).

Buncher

The buncher is a re-entrant cylindrical cavity constructed from a pair of coupling-cavity clamshells (see Fig. 6, Ref. 4). It is operated in the TM_{010} mode with up to 30 watts of power derived from a Moreno cross-guide coupler in the waveguide feed to the pre-accelerator section. Phase adjustment is provided by a motor-driven coaxial-line trombone.

Accelerator Structures

The pre-accelerator structure (called Model 4 for historical reasons) is designed for an increasing velocity, β varying from 0.54 (96 keV) at the input to 0.96 (1.4 MeV) at the output. A common end-wall profile was used for all cells,

the length of the side wall being varied to maintain synchronism. An off-axis bridge coupling cell is placed after the sixth accelerating cell. Five accelerating cells follow the bridge coupler. With 11 coupling cells, the structure has a total of 23 resonant cavities. With the total power in the accelerating cells at 28 kW the design mean energy gradient (excluding the bridge coupler) is 0.8 MeV/m. A more detailed discussion of the design is given in ref. (4) as well as the high-power 100% duty factor performance without beam loading.

The main accelerator tank (Model 3) is similar to the pre-accelerator but designed for β=1. The bridge coupler is placed at the midpoint of 18 identical accelerating cells. With 18 coupling cells, the structure has a total of 37 resonant cavities. The final beam energy will be 4 MeV with 60 kW supplied to the Model 3 structure. Each bridge coupler is driven by a klystron.

The structure has been tested up to 5 kW per cell. As this power density is an order of magnitude greater than that of the LAMPF design, an improved cooling system is required. The ETA accelerator structures are cooled by water flowing in channels milled circumferentially into the copper walls of the cavities. Two channels in each segment provide counter flowing streams to minimize temperature differences along the structure. On the bridge coupler, cooling is provided by axial channels brazed to the outer wall.

Instrumentation for monitoring accelerator parameters includes field probes, thermistors and resistance thermometers (RTD's). Magnetic-coupling field probes are installed in each end cell and every side-coupling cavity is provided with an electric field probe. Thermistors are mounted on each side-coupler, and pairs of RTD's monitor the water temperature rise in each section and on the bridge coupler.

The structures are pumped via manifolds with connections to the side couplers below the beam line. Each manifold also serves as a "strong back". A 400 ℓ/sec ion pump is provided for each tank. The base pressure as indicated by the ion pump current is $\sim 2 \times 10^{-7}$ torr.

Sets of degaussing coils are placed around the injector and accelerator structures to facilitate beam handling. Magnetic gap lenses are used at each end of the tank sections and in the injector beam line. Rectangular box magnets are used for beam steering. Water-cooled quadrant apertures provide protection for the accelerator structures as well as information on beam focussing and positioning.

Following the 90° bend the beam must be diverged with a full angle of 7° so that the power density in the beam dump is reduced to acceptable levels. Using the SLAC "TRANSPORT" program an acceptable solution has been found. This is achieved by a quadrupole followed by a bending magnet with focussing at both input and output edges approaching an approximately achromatic bend (passband 25% in energy) and divergence of 7° in both horizontal and vertical planes.

Control Systems

The control systems are centralized in a control room about 40 feet from the accelerator tunnel. Our design approach has been to provide an independent control system for each major component. This has enabled these components to be commissioned separately. Digital protect circuitry can initiate crowbars, relays, etc., shutting down the gun and rf independently. The frequency, phase and amplitude control systems will also have their own analog control loops.

These systems are gradually being interfaced with a digital computer. This will eventually supervise the control functions of the accelerator. The computer system uses an Interdata Model 70 processor with 40 kbytes of memory, moving head disk, cassette tape, card reader and Computek display. The real time operating system will provide multi-task operation and debugging on-line.

This approach allows us to proceed with the experiment in parallel with the development of more powerful diagnostics and control functions from the computer. The independent approaches will converge as experience with the computer system grows.

Tank Frequency Control (4)

The fields in the three rf structures, the buncher, the graded-β tank and the β=1 tank must have the proper phase and amplitude for acceleration of the beam. The dissipation of heat in the structures at full power causes

resonant frequency changes which are many times the structure bandwidth. The establishment and control of these fields is complicated by the use of multiple rf power sources.

The design power dissipation of 32 kW cw in the graded-β tank causes a frequency shift of 240 kHz at a constant inlet water temperature and a temperature rise of 4°C. At a constant power level the frequency changes linearly with temperature at a rate of 13.7 kHz/°C. Since frequency control is a prerequisite to the solution of many of the operational problems that might be expected in a proton linac, it is in this area that we have devoted much of our effort so far.

Early experiments on frequency control purely by temperature regulation were unsuccessful. With major power level changes, frequency drift rates up to 2 kHz/sec are observed. The tank resonance bandwidth is 34 kHz and the cooling system transport delay is 30 sec. With these parameters a faster frequency control system is required than can be accomplished by coolant temperature control.

Perturbation calculations using a coupled circuit analog (5) indicated that the tank resonance could be controlled safely by detuning a single accelerating cell. No drastic field tilt nor phase shift was predicted by the perturbed model. Consequently, the decision was made to control the tank resonance by means of a tuning plunger in the bridge coupler.

Power is fed through a 9.5 cm diameter circular iris machined into the top of the bridge. Initial static tuning of the bridge coupler was done by a combination of adjusting the size of hemispherically shaped bosses on the bridge end plates and the penetration of a coarse tuning plunger 8.9 cm diameter, mounted horizontally on the outer cylinder wall. The coarse plunger was bored out to allow insertion of a motor driven tuning plunger 6.35 cms in diameter, concentric with the coarse tuner. The motor driven tuner is able to change the bridge frequency by approximately 3 MHz over a travel range of 5 cms. However at a penetration of 2.9 cms (and a bridge frequency change of $\sim$ 2.3 MHz), a parasitic mode is set up in the bridge which is less than 1 MHz from the $\pi/2$ mode frequency. The range of the tuning plunger is therefore restricted to give a $\pi/2$ mode frequency tuning range of 187 kHz.

Table 1 gives the parameters of a coupled circuit analog fit to the dispersion curve for the two limiting positions and the zero position of the tuning plunger. The coupled circuit model correctly predicts that the calculated average accelerating cell frequency should change by the same amount as the measured $\pi/2$ mode frequency. The stop band opens in the expected direction. Although the model is phenomenological in character, these results indicate that it is a useful analog of structure behaviour.

TABLE 1

EFFECT OF BRIDGE TUNER POSITION ON COUPLED CIRCUIT PARAMETERS

Position	$\pi/2$ (Measured) Frequency (MHz)	Accelerating Cell Frequency (MHz)	Side Coupler Cell Frequency (MHz)	Nearest Neighbour Coupling Constant	Second Nearest Neighbour Coupling Constant	Stop Band (MHz)
OUT	804.869	806.913	804.809	0.0452	-0.00510	0.053
ZERO	804.929	806.947	804.798	0.0452	-0.00506	0.116
IN	805.056	807.084	804.719	0.0452	-0.00517	0.287

Tuner Static Tests

A control system based on detuning of the structure requires investigation of the tolerance of the $\pi/2$ mode to large frequency errors in one cell. Experiments were performed with the pre-accelerator structure power dissipation held constant at 33 kW. The motor driven tuner was used to change the $\pi/2$ mode frequency over a range of 180 kHz. Measurements were taken of the accelerating cell fields at the extreme ends of the tank. The field tilt changed by less than 0.7% within the experimental error.

Under the above conditions relative phase measurements were made between probes inserted in the end cells of the structure. Detuning the structure with the plunger, changed the phase by about 0.1° which was comparable with the experimental error. Both results demonstrate the suitability of the $\pi/2$ mode to this type of dynamic tuning procedure.

Table 2 shows the effect of the tuning plunger on fields in the side couplers.

TABLE 2

SENSITIVITY OF COUPLER FIELDS TO PLUNGER POSITION

Coupler Number	Field Difference at Plunger Limits / Field at Plunger mid-Range
1	0.57
3	5.2
4	1.0
5	1.21
8	0.71
9	0.79
10	0.74
11	0.84

Only in coupler 3 and 5 was the field level particularly sensitive to plunger position. The temperature of coupler number 3 was independent of the plunger position at a temperature of $18.5^{\circ}C$ above the inlet water temperature measured near the coupler boss. On the other hand the temperature of coupler 5 increased from $18.5^{\circ}C$ to $23.5^{\circ}C$ above inlet water temperature over the plunger tuning range. This change in temperature was the same when measured at the joint between the coupler and the accelerating structure.

The tests show that the tuning plunger is not responsible for any sizeable perturbations in the accelerating cell fields. Also it may be concluded that side coupler temperatures are determined mainly by the surface temperature of the accelerating structure in the present design.

Dynamic Tests

The tuning plunger does not have sufficient range to keep the graded-β tank on resonance from zero power to 32 kW at a constant frequency. It is therefore used in combination with a water temperature control system which returns the plunger to its set point. Pneumatic control valves regulate the coolant inlet temperature by altering the division of a total constant flow through a heat exchanger and a by-pass.

An error signal proportional to the displacement of the plunger from its set point is derived from a potentiometer coupled to the motor drive shaft. This is fed into an electro-pneumatic transducer to control the pneumatic water flow valves so that the displacement is minimized.

At 32 kW the minimum temperature that can be reached with the present cooling system is $35^{\circ}C$ with the maximum temperature of the service water in summer at $17^{\circ}C$. Consequently tests were carried out with the tank brought to 32 kW at 804.745 MHz and the tuning plunger at the inner limit. Fig. 2 shows the result from one test when the power was decreased from 32 kW to 18 kW. To compensate for the narrow range of our present cooling system the initial conditions were chosen so that the maximum power transient could be supported. The lower curve shows that the plunger moves out as the temperature of the cavity nose cools down. The middle curve shows that to compensate for this the inlet water temperature of the tank increases to keep the tuning plunger at its set point. These preliminary tests demonstrate that mechanical tuning in the bridge coupler can achieve the fast frequency control which is essential in a multi-tank high power accelerator.

Ferrite Isolator

Commissioning of the Model 4 graded-β structure has been facilitated by a ferrite isolator which provides a high isolation at low average power. The isolator was tested with the klystron

delivering power into a flat load. The heat dissipated in the isolator and in the load was measured calorimetrically. The insertion loss falls from 1.6 db at zero power to 0.5 db at 48 kW. With the isolator reversed under the same test conditions the attenuation frops from 17.5 db at low power to 1 db at 45 kW as the ferrite falls out of electron spin resonance at the higher temperature. This deterioration in reverse attenuation is fortunate because large frequency excursions from resonance will not damage the isolator. The klystron is at all times protected with the aid of a signal from a directional coupler immediately in front of the klystron. When reverse power of 45 kW is applied suddenly, a thermal time constant of 9 secs is observed in the decrease of attenuation. This is sufficient time for remedial action to be initiated within the frequency control system.

The performance of the isolator under actual operating conditions is revealed in Fig. 3. The open circles show the reverse attenuation as a function of power absorbed. With a forward power of 36 kW (the operating forward power for Model 4) the insertion loss is responsible for dissipating 4.56 kW. Under these conditions the reverse attenuation is 6.7 db. Higher isolation is usually obtained at the expense of higher insertion loss; the reverse/forward attenuation ratio is plotted in Fig. 3 as solid points. It is expected that the ratio can be improved by optimizing the magnitude and distribution of the magnetic field and the ferrite thickness.

The special merit of this design is apparent during tank commissioning. Multipactor sparks and spurious discharges in the tank when operated under pulsed conditions are prevented from giving reverse power transients at the klystron window. After the cleaning process has progressed and the tank is operated cw the isolator insertion loss drops with the increase in average power. Rf transfer efficiency is therefore increased when the demand for high isolation diminishes.

Beam Tests

A beam of 250 μA has been bunched and accelerated through the Model 4 tank and dumped in a low power Faraday cup installed at the end of the pre-accelerator. Beam current was limited to avoid overheating beam line components. Tests have been carried out with an electrostatic fast beam switch (6) designed so that a shut down of the beam could be accomplished in a few microseconds. The poor beam quality on transmission through this switch has led us to plan for a gun crowbar for fast beam protection.

Buncher

Preliminary tests of the buncher operation were carried out with a bunching detector placed at distances between 50 and 100 cms from the buncher cavity. A single-turn loop around the beam connected through a coaxial cable to a sampling oscilloscope served to display some of the high frequency components in the beam. The loop was protected from direct impact of the beam by a water-cooled aperture. An energy-phase diagram calculated for conditions approximating those of the test is given in Fig. 4. The open circles outline the acceptance area of the accelerator as calculated numerically (7). The dots on the solid curve represent points equally spaced in phase at the centre of the buncher. Fig. 5 shows the normalized current density (bunching factor) as a function of phase. The pickup loop was able to demonstrate the transition from under- to over-bunching and Fig. 6 shows the observed response for the conditions presented in Figs. 4 and 5. Subsequent observations of beam accelerated by the pre-accelerator section showed a gain in transmission 2.5 with buncher operation and verified the buncher parameters found in the preliminary test.

Pre-accelerator Section

For these tests the gun was operated at 90 kV. With the net cw power feed to the structure at 28 kW, the buncher power and phase were adjusted for maximum transmission. Currents up to 250 μA were measured in the Faraday cup. Rough calorimetric measurements on the Faraday cup yielded a beam energy value of 1.24 ± 0.1 MeV. Assuming a synchronous phase angle of 26° (as indicated by trajectory calculations) the observed shunt impedance, ZT^2, is 67.7 ± 8 MΩ. This is consistent with the theoretical value of 88.6 MΩ when an allowance of 20% is made for the effect of coupling slots.

Conclusion

The side-coupled linear accelerator design developed at Los Alamos is stable under 100% duty factor operation at average power levels of 2.5 kW/cell. Such a structure has been used to accelerate a

cw beam of 250 μA and our buncher efficiency and beam energy are consistent with trajectory and mesh calculations.

Our experience shows that water cooling alone would not provide the frequency control necessary for stable operation of a chain of tanks. A non-thermal method to provide dynamic tuning is necessary. We have found that mechanical tuning in the bridge coupler is successful.

Acknowledgements

It is a pleasure to acknowledge the contributions of R.E. Green, H.R. Schneider and A.J. Vale in the early stages of this experiment and to thank S.B. Hodge who was responsible for the mechanical design and fabrication of the tanks together with the klystron and tank cooling systems.

References

(1) The AECL Symposium on the Generation of Intense Neutron Fluxes, AECL-2177 (1965).

(2) "ING Status Report, July 1967" AECL-2750.

(3) B.G. Chidley, S.B. Hodge, J.C. Brown, J.H. Ormrod and J. Ungrin, "The Chalk River High Current Test Facility", Paper at this Conference.

(4) J. McKeown, H.R. Schneider and S.O. Schriber, "High Power Operation of Two Side-Coupled Standing Wave Linac Structures", Paper at this Conference.

(5) D.E. Nagle, E.A. Knapp and B.C. Knapp, R.S.I. 38, 1583 (1967).

(6) James D. Larsen, U.S. Patent 3,558,879 (1971), "Electro-static Deflector for Selectively and Adjustably Bending a Charged Particle Beam".

(7) B. Austin, T.W. Edwards, J.E. O'Meara, M.L. Palmer, D.A. Swenson and D.E. Young, "The Design of Proton Linear Accelerators", MURA-715, (1965).

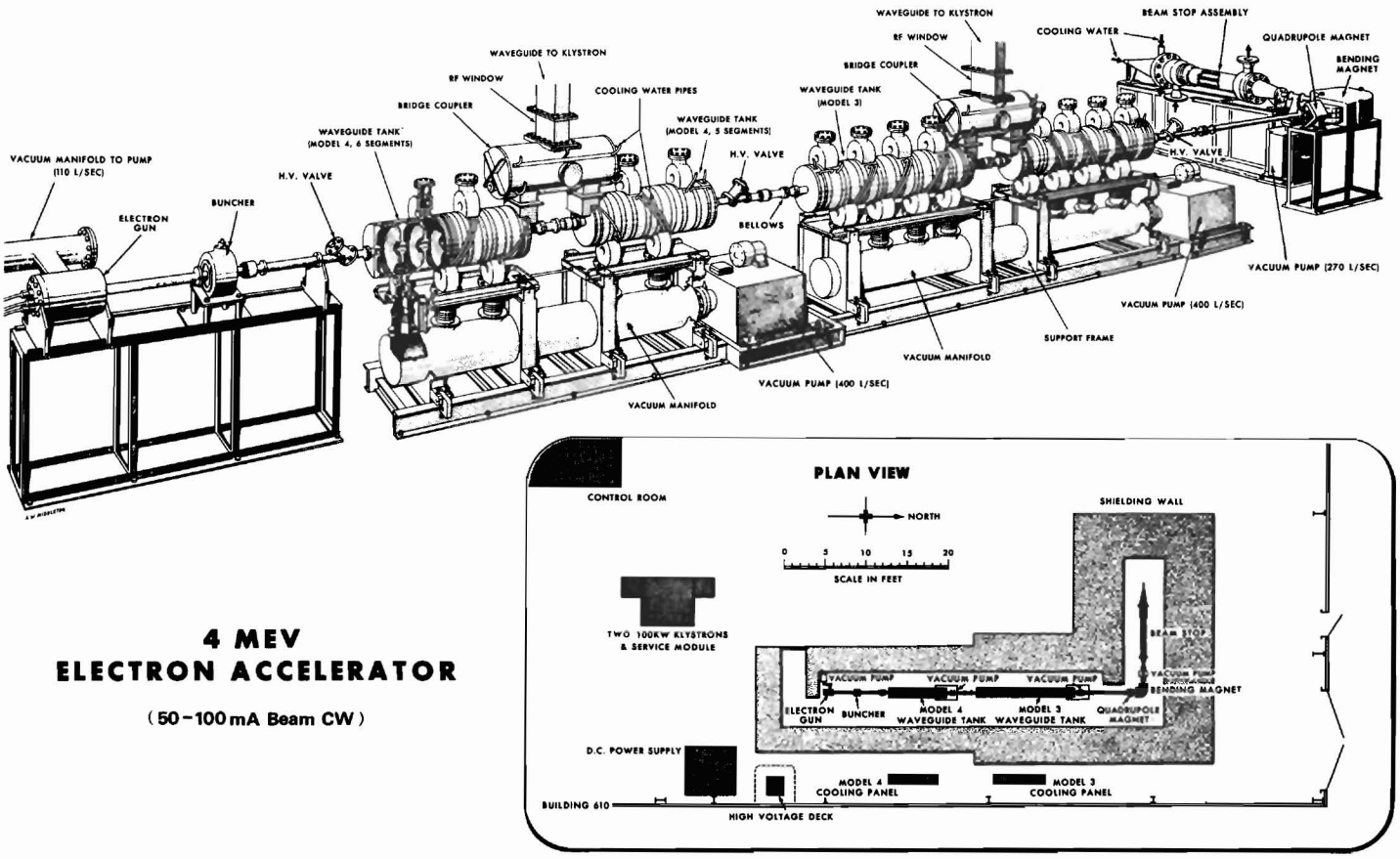

Fig. 1. Isometric view of the accelerator

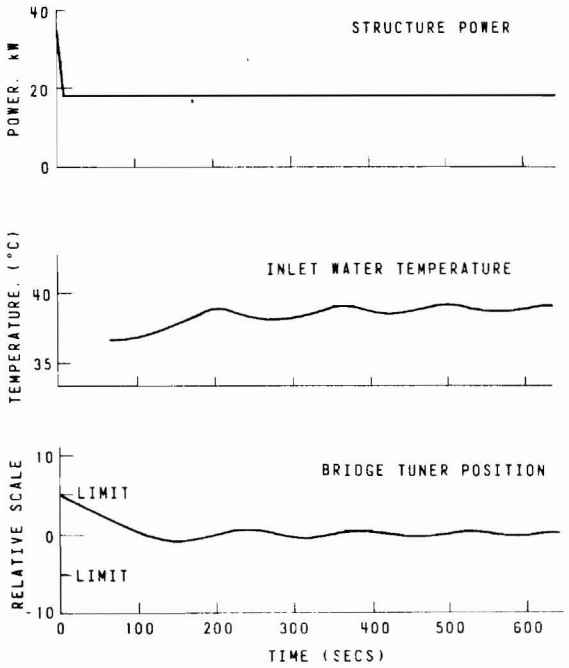

Fig. 2. Response of resonance control system to power transient at fixed frequency

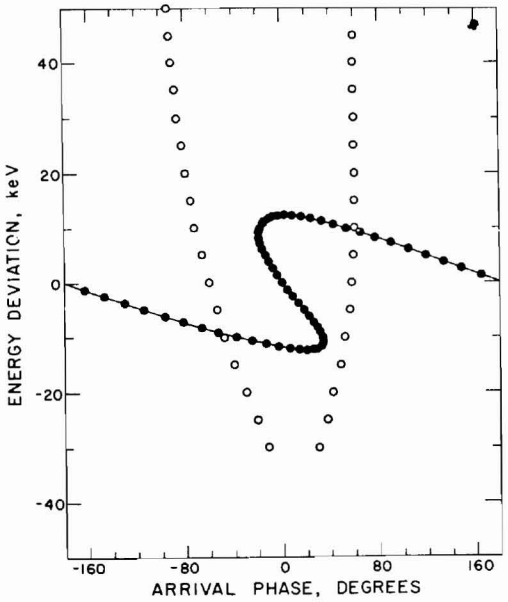

Fig. 4. Energy-phase diagram for the buncher. Beam energy 90 keV, peak buncher voltage 15 kV, drift distance 100 cm

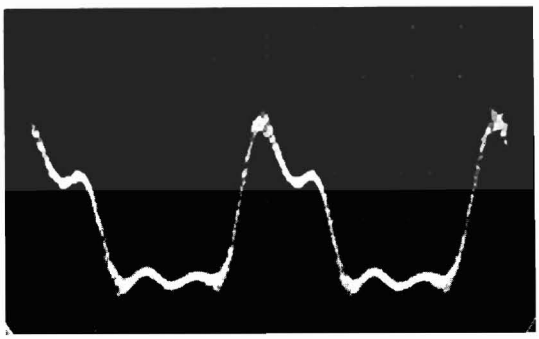

Fig. 6. Observed response of beam pick-up loop

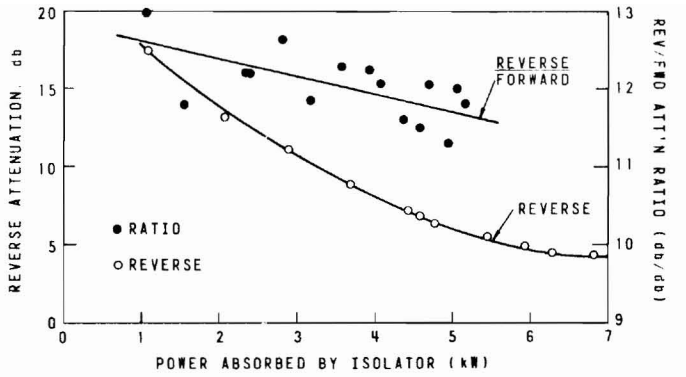

Fig. 3. Reverse attenuation and reverse/forward attenuation ratio as a function of isolator absorbed power

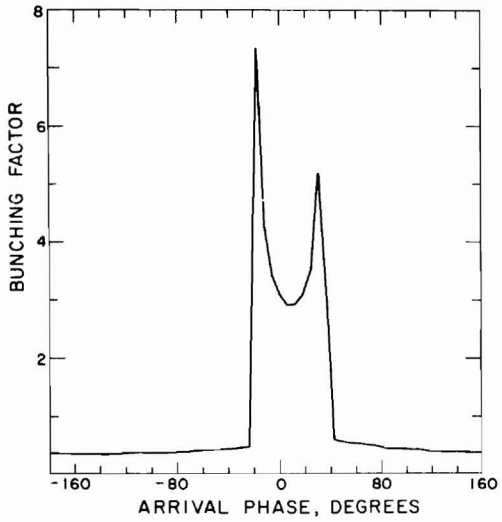

Fig. 5. Bunching factor for the same conditions as for Fig. 4

DISCUSSION

Blewett, BNL: Why did you use the bridge coupler to avoid knife-edge seals?

Fraser, AECL: It was a personal preference for brazed connections.

Allen, SLAC: If you did not use the bridge coupler, would you have tuned the on-line cavities directly?

Fraser: We considered this, but it is safer to do the tuning in the bridge coupler to avoid perturbing the fields on the axis.